Biochimica et Biophysica Acta xxx (2010) xxx–xxx

Contents lists available at ScienceDirect

Biochimica et Biophysica Acta

journal homepage: www.elsevier.com/locate/bbamem

Interaction of the N-terminal segment of HCV protein NS5A with model membranes

M. Francisca Palomares-Jerez [a], Jaime Guillén [b], José Villalaín [a,*]

[a] Instituto de Biología Molecular y Celular, Universidad Miguel Hernández, E-03202 Elche-Alicante, Spain
[b] Departamento de Bioquímica y Biología Molecular A, Universidad de Murcia, E-30080 Espinardo, Murcia, Spain

ARTICLE INFO

Article history:
Received 3 December 2009
Received in revised form 18 January 2010
Accepted 4 February 2010
Available online xxxx

Keywords:
HCV
NS5A
Model membrane

ABSTRACT

We have identified a membrane-active region in the HCV NS5A protein by performing an exhaustive study of membrane rupture induced by a NS5A-derived peptide library on model membranes having different phospholipid compositions. We report the identification in NS5A of a highly membranotropic region located at the suggested membrane association domain of the protein. We report the binding and interaction with model membranes of two peptides patterned after this segment, peptides 1A and 1B, derived from the strains 1a_H77 and 1b_HC-4J respectively. We show that they insert into phospholipid membranes, interact with them, and are located in a shallow position in the membrane. The NS5A region where this segment resides might have an essential role in the membrane replication and/or assembly of the viral particle through the modulation of the replication complex, and consequently, directly implicated in the HCV life cycle.

1. Introduction

The enveloped positive single-stranded RNA hepatitis C virus (HCV), classified in the genus *Hepacivirus* within the family *Flaviviridae*, is the major cause of liver disease. With an estimated 170 to 200 million people infected worldwide [1], its high persistence, no protective vaccine available at present and limited current therapeutic agents, this disease has emerged as a serious healthcare problem on a global scale [2]. The variability of the HCV proteins gives the virus the ability to escape the host immune surveillance system and notably hampers the development of an efficient vaccine.

HCV has a single-stranded genome which encodes a polyprotein of about 3010 amino acids, which is cleaved by a combination of cellular and viral proteases to produce the mature proteins [3]. HCV entry into the host cell is achieved by the fusion of viral and cellular membranes, its replication cycle is highly dependent on host cell lipids, and the morphogenesis has been suggested to take place in the endoplasmic reticulum [4]. Details about HCV replication process remain largely unclear, but most if not all of the HCV non-structural proteins (NS) proteins are involved [3]. NS proteins include two viral proteases, NS2 and NS3, responsible for the maturation of all the NS proteins [5]. NS3 is a multifunctional protein with a RNA helicase/NTPase domain apart from the serine protease domain [6]. The NS4A protein, an integral membrane protein, which is predicted to contain at least four transmembrane domains, serves as a cofactor for NS3 and is incorporated as an integral component into the enzyme core. NS4B is an integral membrane protein which seems to be implicated in the formation of the replication complex within the endoplasmic reticulum membranes [7], as well as is also engaged in virus assembly and release [8]. The NS5B RNA-dependent RNA polymerase is the catalytic subunit of the viral replication complex [9].

NS5A is a membrane-anchored phosphoprotein which is indispensable for replication, essential for efficient virus assembly and has been suggested to be involved in interferon resistance and apoptotic regulation [10–12]. Although numerous functions have been suggested for NS5A, its ultimate function/s in the HCV life cycle is/are not known. However, NS5A is an absolutely required component of the viral replicase and has been recognised as a promising therapeutic target [13]. NS5A contains three domains, and has been observed in two forms, phosphorylated and hyper-phosphorylated [14]. It has been shown that domain I has a tight association with the membrane, association mediated post-translationally by a segment within the N-terminal fragment of NS5A [15] (Fig. 1A). This segment has been proposed to be an amphipathic α-helix [16,17]. The helix defines a

Abbreviations: 16-NS, 16-doxyl-stearic acid; 5-NS, 5-doxyl-stearic acid; BPI, bovine brain L-α-phosphatidylinositol; BPS, bovine brain L-α-phosphatidylserine; CF, 5-carboxyfluorescein; Chol, cholesterol; CL, bovine heart cardiolipin; di-8-ANEPPS, 4-(2-(6-(dioctylamino)-2-naphthalenyl)-(ethenyl)-1-(3-sulfopropyl)-pyridinium inner salt; DMPA, 1,2-dimyristoyl-sn-glycero-3-phosphatidic acid; DMPC, 1,2-dimyristoyl-sn-glycero-phosphatidylcholine; DMPG, 1,2-dimyristoyl-sn-glycero-phosphatidylglycerol; DMPS, 1,2-dimyristoyl-sn-glycero-3-phosphatidylserine; DPH, 1,6-diphenyl-1,3,5-hexatriene; DSC, differential scanning calorimetry; EPA, egg L-α-phosphatidic acid; EPC, egg L-α-phosphatidylcholine; ER, endoplasmic reticulum; ESM, egg sphingomyelin; FD10, fluorescein isothiocyanate dextran with an average molecular weight of 10,000; HCV, hepatitis C virus; LUV, large unilamellar vesicles; MLV, multilamellar vesicles; NS, non-structural protein; TFE, trifluoroethanol; T_m, temperature of the gel-to-liquid crystalline phase transition; TM, transmembrane domain; TMA-DPH, 1-(4-trimethylammoniumphenyl)-6-phenyl-1,3,5-hexatriene; TPE, egg trans-esterified L-α-phosphatidylethanolamine

* Corresponding author. Tel.: +34 966 658 762; fax: +34 966 658 758.
E-mail address: jvillalain@umh.es (J. Villalaín).

0005-2736/$ – see front matter © 2010 Elsevier B.V. All rights reserved.
doi:10.1016/j.bbamem.2010.02.007

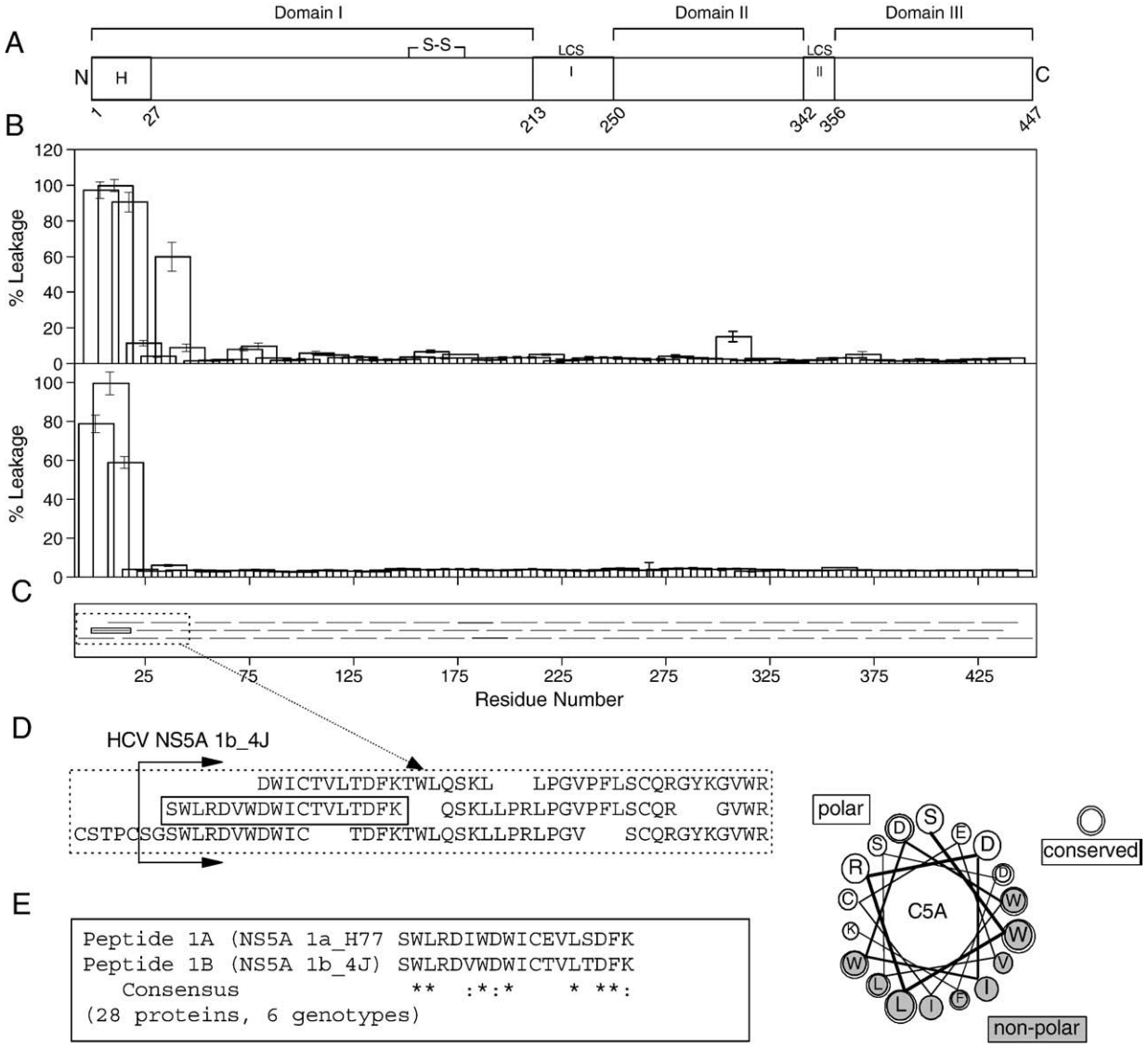

Fig. 1. (A) Schematic representation of HCV NS5A protein showing the proposed location of domains I, II and III, the low-complexity sequences (LCS) I and II, as well as the amino terminal amphipathic helix [61]. Numbers refer to amino acid numbering of NS5A 1b_HC-J4. (B) Membrane leakage elicited by the HCV NS5A 1b_HC-J4 peptide library on model membranes composed of EPC/ESM/Chol at a phospholipid molar ratio of 5:1:1, and a complex lipid composition resembling the ER membrane (upper and lower histograms, respectively). Vertical bars indicate standard deviations of the mean of triplicate samples. (C) Relative location of the 64 18-mer peptides derived from the HCV NS5A 1b_HC-J4 protein is shown with respect to the sequence of the protein. Maximum overlap between adjacent peptides is 11 amino acids. (D) Correlation of the HCV NS5A-derived peptide library with the peptide library and sequences of the peptides 1A and 1B used in this study. (E) Sequence of the NS5A peptides 1A and 1B used in this work, along the consensus sequence obtained using twenty-eight NS5A sequences from the six main HCV genotypes.

platform probably involved in specific protein–protein interactions essential for the formation of a functional HCV replication complex [18]. The introduction of mutations into the hydrophobic face of the N-terminal segment of NS5A has a critical consequence that generate the inhibition of HCV RNA replication, hence the importance of the segment-membrane association for the viral life cycle [19]. Interestingly, an amphipathic helical peptide derived from the N-terminal fragment of NS5A has been shown to be virocidal against HCV [20].

Previous studies from our group studying the effect of glycoprotein-derived peptide libraries on model membrane integrity have helped us to understand the mechanisms underlying the interaction between viral proteins and membranes [21–23]. In the present study, we report the binding and interaction of two peptides corresponding to the N-terminal segment of protein NS5A from two strains, namely 1a_H77 and 1b_HC-J4, and define it as a membrane interacting domain. We show that this segment strongly partitions into phospholipid membranes, interacts with them, and is located in a shallow position in the membrane. These results would suggest that this NS5A element is an essential constituent of the interaction between the protein and the membrane and might shed light into the specific function of the NS5A protein in the viral cycle.

2. Materials and methods

2.1. Materials and reagents

One set of 64 peptides derived from the HCV 1b_HC-J4 NS5A protein was obtained through the NIH AIDS Research and Reference Reagent Program (Division of AIDS, NIAID, NIH, Bethesda, MD). Peptides 1A (HCV strain 1a_H77, sequence ^{3}SWLRDIWDWICEVLSDFK^{20}) and 1B (HCV strain 1b_HC-J4, sequence ^{3}SWLRDVWDWICTVLTDFK^{20}) were synthesized with N-terminal acetylation and C-terminal amidation on an automatic multiple synthesizer (Genemed Synthesis, San Antonio, TX, USA). The peptides were purified by reverse-phase high-performance

Please cite this article as: M.F. Palomares-Jerez, et al., Interaction of the N-terminal segment of HCV protein NS5A with model membranes, Biochim. Biophys. Acta (2010), doi:10.1016/j.bbamem.2010.02.007

liquid chromatography (Vydac C-8 column, 250×4.6 mm, flow rate 1 ml/min, solvent A, 0.1% trifluoroacetic acid, solvent B, 99.9 acetonitrile and 0.1% trifluoroacetic acid) to >95% purity, and its composition and molecular mass were confirmed by amino acid analysis and mass spectrometry. Since trifluoroacetate has a strong infrared absorbance at approximately 1673 cm^{-1}, which interferes with the characterization of the peptide Amide I band [24], residual trifluoroacetic acid, used both in peptide synthesis and in the high-performance liquid chromatography mobile phase, was removed by several lyophilisation/solubilisation cycles in 10 mM HCl [25]. Peptides were solubilized in water/TFE at 50% v/v). Bovine brain phosphatidylserine (BPS), bovine liver L-α-phosphatidylinositol (BPI), cholesterol (Chol), egg phosphatidic acid (EPA), egg L-α-phosphatidylcholine (EPC), egg sphingomyelin (ESM), egg trans-esterified L-α-phosphatidylethanolamine (TPE), tetramyristoyl cardiolipin (CL), 1,2-dimyristoylphosphatidylserine (DMPS), 1,2-dimyristoylphosphatidic acid (DMPA), 1,2-dimyristoylphosphatidylcholine (DMPC) and 1,2-dimyristoylphosphatidylglycerol (DMPG) were obtained from Avanti Polar Lipids (Alabaster, AL, USA). The lipid composition of the synthetic endoplasmic reticulum was EPC/CL/BPI/TPE/BPS/EPA/ESM/Chol at a molar ratio of 59:0.37:7.7:18:3.1:1.2:3.4:7.8 [26]. 5-Carboxyfluorescein (CF, >95% by HPLC), 4-(2-(6-(dioctylamino)-2-naphthalenyl)ethenyl)-1-(3-sulfopropyl)-pyridinium inner salt (di-8-ANEPPS), 5-doxyl-stearic acid (5-NS), 16-doxyl-stearic acid (16-NS), fluorescein isothiocyanate labeled dextran FD-10, deuterium oxide (99.9%), Triton X-100, EDTA and HEPES were purchased from Sigma-Aldrich (Madrid, ES). 1,6-Diphenyl-1,3,5-hexatriene (DPH), and 1-(4-trimethylammoniumphenyl)-6-phenyl-1,3,5-hexatriene (TMA-DPH) were obtained from Molecular Probes (Eugene, OR). All other chemicals were commercial samples of the highest purity available (Sigma-Aldrich, Madrid, ES). Water was deionized, twice-distilled and passed through a Milli-Q equipment (Millipore Ibérica, Madrid, ES) to a resistivity higher than 18 MΩ cm.

2.2. Vesicle preparation

Aliquots containing the appropriate amount of lipid in chloroform–methanol (2:1 vol/vol) were placed in a test tube, the solvents were removed by evaporation under a stream of O_2-free nitrogen, and finally, traces of solvents were eliminated under vacuum in the dark for >3 h. The lipid films were resuspended in an appropriate buffer and incubated either at 25 °C or 10 °C above the phase transition temperature (T_m) with intermittent vortexing for 30 min to hydrate the samples and obtain multilamellar vesicles (MLV). The samples were frozen and thawed five times to ensure complete homogenization and maximization of peptide/lipid contacts with occasional vortexing. Large unilamellar vesicles (LUV) with a mean diameter of 0.1 μm (leakage measurements) and 0.2 μm (dextran release assays) were prepared from MLV by the extrusion method [27] using polycarbonate filters with a pore size of 0.1 and 0.2 μm (Nuclepore Corp., Cambridge, CA, USA). For infrared spectroscopy, aliquots containing the appropriate amount of lipid in chloroform/methanol (2:1, v/v) were placed in a test tube containing 200 μg of dried lyophilized peptide. After vortexing, the solvents were removed by evaporation under a stream of O_2-free nitrogen, and finally, traces of solvents were eliminated under vacuum in the dark for more than three hours. The samples were hydrated in 100 μl of D_2O buffer containing 20 mM HEPES, 100 mM NaCl, 0.1 mM EDTA, pH 7.4 and incubated at 10 °C above the T_m of the phospholipid mixture with intermittent vortexing for 45 min to hydrate the samples and obtain MLV. The samples were frozen and thawed as above. Finally the suspensions were centrifuged at 15,000 rpm at 25 °C for 15 min to remove the possibly peptide unbound to the membranes. The pellet was resuspended in 25 μl of D_2O buffer and incubated for 45 min at 10 °C above the T_m of the lipid mixture, unless stated otherwise. The phospholipid and peptide concentration were measured by methods described previously [28,29].

2.3. Membrane leakage and peptide binding to vesicles

LUVs with a mean diameter of 0.1 μm were prepared as indicated above in buffer containing 10 mM Tris, 20 mM NaCl, pH 7.4, and CF at a concentration of 40 mM. Non-encapsulated CF was separated from the vesicle suspension through a Sephadex G-75 filtration column (Pharmacia, Uppsala, SW, EU) eluted with buffer containing 10 mM Tris, 100 mM NaCl, and 1 mM EDTA, pH 7.4. Membrane rupture (leakage of intraliposomal CF) was assayed by treating the probe-loaded liposomes (final lipid concentration, 0.125 mM) with the appropriate amounts of peptide on microtiter plates using a microplate reader (FLUOstar; BMG Labtech, Offenburg, Germany), stabilized at 25 °C with the appropriate amounts of peptide, each well containing a final volume of 170 μl. The medium in the microtiter plates was continuously stirred to allow the rapid mixing of peptide and vesicles. In the case of LUVs (0.2 μm) encapsulated with fluorescent dextran FD10, the lipid was resuspended to a concentration of 100 mg/ml solution of dextrans in buffer containing 10 mM Tris, 100 mM NaCl, pH 7.4. Non-encapsulated dextrans were removed by gel-filtration chromatography using a pump P-50 (Amershan Pharmacia Biotech AB, Uppsala, Sweden) with a Sephacryl® 500-HR column eluted with the same buffer above described, at a flow rate of 3 ml/min. The final lipid concentration was 0.075 mM in a 5 mm×5 mm fluorescence cuvette (final volume of 400 μl), stabilized at 25 °C and under constant stirring. Fluorescence was measured using a Varian Cary Eclipse spectrofluorimeter. One hundred percent release was achieved by adding Triton X-100 to either the microtiter plate or the cuvette to final concentration of 0.5% (w/w). Changes in fluorescence intensity were recorded with excitation and emission wavelengths set at 492 and 517 nm, respectively. Excitation and emission slits were set at 5 nm. Leakage was quantified on a percentage basis as previously described [30,31]. The mole fraction partition coefficient K_p, i.e., the amount of peptide in the bilayer as a fraction of the total peptide present in the system, was evaluated by the enhancement of the tryptophan fluorescence by successive additions of small volumes of LUV to a peptide sample (2.15×10^{-5} M) as described previously [32]. Fluorescence spectra were recorded in a SLM Aminco 8000C spectrofluorometer with excitation and emission wavelengths of 290 and 348 nm, respectively, and 4 nm spectral bandwiths. Measurements were carried out in 10 mM Tris, 100 mM NaCl, and EDTA 0.1 mM, pH 7.4. Intensity values were corrected for dilution, and the scatter contribution was derived from lipid titration of a vesicle blank.

2.4. Acrylamide quenching of Trp emission, quenching with lipophylic depth probes and steady-state fluorescence anisotropy

Aliquots from a 4 M solution of the water-soluble quencher were added to the solution-containing peptide in the presence and absence of liposomes at a peptide/lipid molar ratio of 1:100. The results obtained were corrected for dilution and the scatter contribution was derived from acrylamide titration of a vesicle blank. Aliquots of TMA-DPH or DPH in N,N′-dimethylformamide were directly added into MLVs formed in 10 mM Tris, 100 mM NaCl, EDTA 0.1 mM, pH 7.4 to obtain a probe/lipid molar ratio of 1/500. Samples were incubated for 15 or 60 min when TMA-DPH or DPH were used, respectively, 10 °C above the gel to liquid crystalline phase transition temperature T_m of the phospholipid mixture. Afterwards, the peptides were added to obtain a peptide/lipid molar ratio of 1:15 and incubated 10 °C above the T_m of each lipid for one hour, with occasional vortexing. All fluorescence studies were carried using 5 mm×5 mm quartz cuvettes in a final volume of 400 μl (315 μM lipid concentration). The steady-state fluorescence anisotropy was measured with an automated polarization accessory using a Varian Cary Eclipse fluorescence spectrometer, coupled to a Peltier for automatic temperature change. Samples were excited at 360 nm (slit width, 5 nm) and fluorescence

Please cite this article as: M.F. Palomares-Jerez, et al., Interaction of the N-terminal segment of HCV protein NS5A with model membranes, Biochim. Biophys. Acta (2010), doi:10.1016/j.bbamem.2010.02.007

emission was recorded at 430 nm (slit width, 5 nm). Quenching studies with lipophylic probes were performed by successive addition of small amounts of 5-NS or 16-NS in ethanol to peptide samples incubated with LUV. The final concentration of ethanol was kept below 2.5% (v/v) to avoid any significant bilayer alterations. After each addition an incubation period of 15 min was kept before the measurement. The data were analyzed as previously described [31]. The Stern–Volmer quenching constant, K_{sv}, obtained from the Stern–Volmer equation, represents the quencher concentration at which 50% of the intensity is quenched and it is therefore a measure of the accessibility of Trp to the quencher molecule [33].

2.5. Measurement of the membrane dipole potential using Di-8-ANEPPS-labeled membranes

Aliquots containing the appropriate amount of lipid in chloroform–methanol (2:1 vol/vol) and di-8-ANEPPS were placed in a test tube to obtain a probe/lipid molar ratio of 1/100 and LUVs, with a mean diameter of 90 nm, were prepared as described previously. Steady-state fluorescence measurements were recorded with a Varian Cary Eclipse spectrofluorimeter. Dual wavelength recordings with the dye di-8-ANEPPS were obtained by exciting the samples at two different wavelengths (450 and 520 nm) and measuring their intensity ratio, R(450/520), at an emission wavelength of 620 nm [34,35]. Changes in the total membrane dipole moment cause a shift in the excitation spectrum maximum of di-8-ANEPPS. The lipid concentration was 200 μM, and all experiments were performed at 25 °C.

2.6. Differential scanning calorimetry

MLVs were formed as stated above in 20 mM HEPES, 100 mM Na Cl, 0.1 mM EDTA, pH 7.4. The peptide was added to obtain a peptide/lipid molar ratio of 1:15. The final volume was 1.2 ml (0.5 mM lipid concentration), and incubated 10 °C above the T_m of each phospholipid for 1 h with occasional vortexing. Samples were loaded into the calorimetric cell. DSC experiments were performed in a VP-DSC differential scanning calorimeter (MicroCal LLC, MA) under a constant external pressure of 30 psi in order to avoid bubble formation, and samples were heated at a constant scan rate of 60 °C/h. Experimental data were corrected from small mismatches between the two cells by substracting a buffer baseline prior to data analysis. The excess heat capacity functions were the analyzed by using Origin 7.0 (Microcal Software). The thermograms were defined by the onset and completion temperatures of the transition peaks obtained from heating scans. In order to avoid artifacts due to the thermal history of the sample, the first scan was never considered; second and further scans were carried out until a reproducible and reversible pattern was obtained.

2.7. Magic angle spinning (MAS) ^{31}P NMR

Samples were prepared as described above and concentrated by centrifugation (14,000 rpm for 15 min). MAS ^{31}P NMR spectra were acquired on a Bruker 500 MHz Avance spectrometer (Bruker BioSpin, Rheinstetten, Germany) using a Bruker 4-mm broad band MAS probe under both static and MAS conditions. The samples were packed into 4-mm zirconia rotors and placed in the spinning module of the MAS probe; no cross-polarization was used. The spinning speed was 10 kHz, regulated to ±3 Hz by a Bruker pneumatic unit and the temperature was 15 °C. A single ^{31}P 90° pulse (typically 5 μs) was used for excitation, a gated broadband decoupling of 10 W, 32 k data points, 3600 transients and 3 s delay time between acquisitions. Under static conditions, the samples showed a broad asymmetrical signal with a low-frequency peak and a high-frequency shoulder characteristic of bilayer structures (data not shown).

2.8. Infrared spectroscopy

Approximately 25 μl of a pelleted sample in D_2O was placed between two CaF_2 windows separated by 50-μm thick Teflon spacers in a liquid demountable cell (Harrick, Ossining, NY). The spectra were obtained in a Bruker IFS55 spectrometer using a deuterated triglycine sulfate detector. Each spectrum was obtained by collecting 200 interferograms with a nominal resolution of 2 cm^{-1}, transformed using triangular apodization and, in order to average background spectra between sample spectra over the same time period, a sample shuttle accessory was used to obtain sample and background spectra. The spectrometer was continuously purged with dry air at a dew point of −40 °C in order to remove atmospheric water vapour from the bands of interest. All samples were equilibrated at the lowest temperature for 20 min before acquisition. An external bath circulator, connected to the infrared spectrometer, controlled the sample temperature. For temperature studies, samples were scanned using 2 °C intervals and a 2-min delay between each consecutive scan. The data were analyzed as previously described [30,36].

3. Results

HCV NS5A protein is a 447 amino acid phosphoprotein, which is divided into three domains interconnected by two connecting loops (Fig. 1A). The NS5A sequence comprising amino acids 1 to 27 corresponds to the proposed amphipathic α-helix which should mediate membrane in-plane association of the protein to the membrane [15–17]. Additionally, a peptide corresponding to amino acid sequence from 3 to 20 of genotype 1a HCV NS5A has been shown to destabilize membranes as well as present virocidal activity against HCV [20]. In order to find any sequence within NS5A which might interact with the membrane, we have studied the effect of a HCV 1b_HC-J4 NS5A-derived peptide library on membrane rupture by monitoring the CF leakage from two different liposome compositions. The first one has been the lipid mixture composed of EPC/ESM/Chol at a phospholipid molar ratio of 5:1:1, and the second one resembles the ER membrane (EPC/CL/BPI/TPE/BPS/EPA/ESM/Chol at a molar ratio of 59:0.37:7.7:18:3.1:1.2:3.4:7.8, [26]). The peptide library used in this study and their correlation with the HCV NS5A protein sequence is depicted in Fig. 1C. Two and three consecutive peptides in the library have an overlap of 11 and 4 amino acids, respectively. Note that the NS5A-derived peptides include the whole HCV NS5A protein sequence (residues 1 to 447, NS5A numbering). When the NS5A-derived peptides were assayed on liposomes, some exerted an important leakage effect as seen in Fig. 1B. The most remarkable effect was observed for the first three peptides in the library, i.e., peptides comprising amino acid residues from −5 to 13, from 3 to 20 and from 10 to 27 (Fig. 1D). These peptides produced leakage values for both types of liposomes between 60 and 100%, depending on the specific lipid composition of the liposomes (Fig. 1B). It is interesting to note that, apart from these three peptides, no significant leakage was elicited for any other of the peptides in both liposome systems (Fig. 1B). Peptide comprising amino acids 3 to 20, which completely disrupted both types of membranes, posses common hydrophobic and hydrophilic positions for all HCV genotypes, demonstrating its amphipathic nature (Table 1 and [37]). Taking into account these results, as well as the above mentioned literature data concerning the membrane-mediated HCV replication process which involve many if not all of the HCV NS proteins, we have performed an in-depth study of the interaction of the NS5A segment comprising residues 3 to 20 with membrane model systems. In order to discern any differences between related sequences of NS5A proteins, we have studied two peptides from genotypes 1a_H77 HCV NS5A (peptide 1A) and 1b_HC-J4 HCV NS5A (peptide 1B) (their sequences are displayed in Fig. 1E). We have investigated their binding and interaction with different membrane model systems, as well as characterized the structural

Please cite this article as: M.F. Palomares-Jerez, et al., Interaction of the N-terminal segment of HCV protein NS5A with model membranes, Biochim. Biophys. Acta (2010), doi:10.1016/j.bbamem.2010.02.007

Table 1
Alignment (clustalw2) for reference strains representing the major genotypes of hepatitis C virus. Alignment of residues 3–20 (HCV NS5A numbering) is only shown. The consensus sequence is shown beneath the alignment. Symbols * and : stand for identical and highly conserved residues, respectively. The sequences studied in this work are emphasized in bold.

Genotype and strain	Sequence
1a_H77	**SWLRDIWDWICEVLSDFK**
1c_HC-G9	SWLKDVWDWICEVLSDFK
6h_VN004	SWLRDIWDWVCEVLSDFK
6a_6a33	SWLRDVWDWVCTVLSDFK
6b_Th580	SWLRDVWDWVCTVLSDFK
6t_D49	SWLRDVWDWVCTVLSDFK
6d_VN235	SWLKDVWDWVCTVLSDFK
6e_D42	SWLRDVWDWVCMVLSDFK
4f_CM_DAV9905	SWLWEIWDWVCTVLSDFK
4d_24	SWLWEIWDWVCTVLSDFK
4a_ED43	SWLWEVWDWVLHVLSDFK
1g_1804	SWLSEIWDWICTVLSDFK
4k_PB65185	SWLREVWDWVCTVLTDFK
6c_Th846	TWLREVWDWVCTVLSDFK
1b_Con1	SWLRDVWDWICTVLTDFK
1b_HC-J4	**SWLRDVWDWICTVLTDFK**
2i_D54	SWLWDVWDWICSILTDFK
2c_BEBE1	SWLRDVWDWVCSILIDFK
2a_HC-J6	SWLRDVWDWVCTILTDFK
2k_VAT96	SWLRDIWDWACTILTDFK
6o_D85	SWLRDIWDWVCTVLSDFK
6f_C-0044	SWLRDIWDWVCTVLSDFK
6k_VN405	SWLRDIWDWVCTVLSDFK
6g_JK046	TWLRDIWDWVCTVLSDFR
5a_EUH1480	TWLRAIWDWVCTALTDFK
3a_NZL1	DWLRTIWDWVCSVLADFK
3b_Tr-Kj	DWLHDIWDWVCIVLSDFK
3k_JK049	NWLYDIWNWVCTVLADFK
Consensus	** .*.* * **:

changes taking place in both the peptides and the phospholipid molecules.

The ability of the NS5A 1A and 1B peptides to interact with membranes was determined from fluorescence studies of the peptide intrinsic Trp residues in presence of model membranes [38] containing different phospholipid compositions at different lipid/peptide ratios (Fig. 2). In order to observe any specific interaction of the peptides with any specific type of lipid, the model membranes were composed of zwitterionic and negatively charged phospholipids as well as SM and Chol at different molar ratios. The presence of both SM and Chol has been related to the occurrence of laterally segregated membrane microdomains or "lipid rafts". Interestingly, it has been shown that active replication complexes of HCV might be localized in lipid rafts [39,40]. The change in the Trp fluorescent spectral properties in the presence of phospholipids indicates that the peptides interact with these model membranes. The Trp fluorescence intensity of both peptides increased upon increasing the lipid/peptide ratio, indicating a significant change on the environment of the Trp moiety of the peptides (Fig. 2A and B). For both peptides, partition constant (K_p) values in the range 10^5 were obtained for the different phospholipid compositions studied (Table 2), indicating that the peptides were bound to the membrane with high affinity [38,41]. Interestingly, differences in fluorescence intensity were also observed, since the increase of intensity was higher in zwitterionic membranes than in the presence of model membranes containing the negatively charged phospholipid BPS (Fig. 2). Differences in the fluorescence anisotropy values of the peptides were also observed in the presence of phospholipid model membranes. It was found that addition of liposomes to the 1A and 1B peptides increased significantly the Trp anisotropy values (from about 0.06–0.07 in solution to a limiting value of 0.19–0.22 in the presence of membranes), indicating a significant motional restriction of the Trp moieties of the peptides at a relatively high lipid/peptide ratio. The NS5A 1A and 1B peptides have

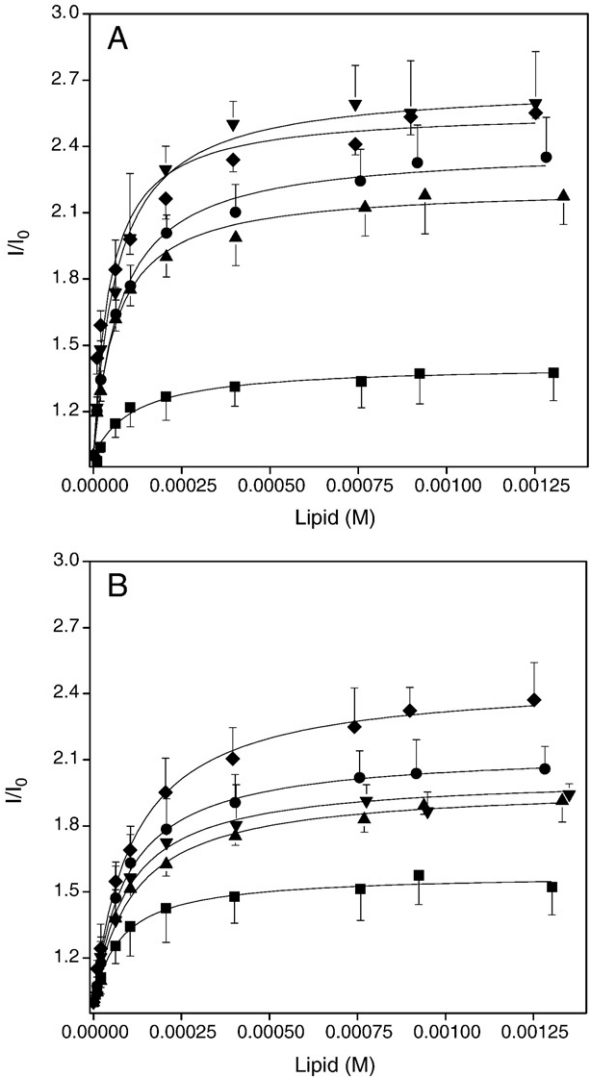

Fig. 2. Change on the fluorescence intensity of the Trp residues of the NS5A-derived peptides 1A (A) and 1B (B) in the presence of increasing lipid concentrations. The lipid compositions used were EPC/ESM/CHOL at a molar ratio of (5:1:1) (●), EPC/CHOL at a molar ratio of 5:1 (▲), synthetic ER membranes (▼), BPS/CHOL at a molar ratio of 5:1 (■) and EPC (◆). Vertical bars indicate standard deviations of the mean of triplicate samples.

a negative net formal charge of −2 and −1 respectively, so it is reasonable to assume that an electrostatic repulsion with membranes composed of negatively charged phospholipids modulates the location of the peptides in the membrane. Because of this, the increase of Trp fluorescence in the presence of anionic membranes is lower than in the presence of membranes containing zwitterionic phospholipids.

To explore the effect of the NS5A peptides 1A and 1B in the destabilization of membrane vesicles, we studied their effect on the release of the encapsulated fluorophores CF and FD10 (Stokes radius around 6 Å and 23 Å, respectively) in model membranes [42,43]. The extent of CF leakage observed at different peptide to lipid molar ratios and the effect on different phospholipid compositions is shown in Fig. 3A and B, where it can be seen that the peptides were able to induce the release of the internal contents of the liposomes in a dose-dependent manner. It is interesting to note that the NS5A 1A and 1B peptides induced a high percentage of leakage (60–90%), even at lipid/peptide ratios as high as 30:1, for liposome compositions of EPC/Chol at molar ratios of 5:1 and 5:3, EPC/ESM/Chol at molar ratios of 5:1:1 and 5:3:1, and EPC (Fig. 3A). In the case of the ER complex

Please cite this article as: M.F. Palomares-Jerez, et al., Interaction of the N-terminal segment of HCV protein NS5A with model membranes, Biochim. Biophys. Acta (2010), doi:10.1016/j.bbamem.2010.02.007

Table 2
Partition coefficients, Stern–Volmer quenching constants and maximal leakage values for the NS5A 1A and 1B peptides incorporated in LUVs of different compositions.

	Peptide	1A	1B	1A	1B	1A	1B	1A	1B	1A	1B	1A	1B
		K_p ($\times 10^{-5}$ M^{-1}) Trp		K_{sv} (M^{-1}) acrylamide		K_{sv} (M^{-1}) 5-NS		K_{sv} (M^{-1}) 16-NS		CF leakage (max%)		FD10 leakage (max%)	
LUV compositions	EPC	4.77 ± 0.62	2.16 ± 0.32	1.29	1.87	22.38	27.89	5.01	9.26	87	65	89	96
	ER	2.88 ± 0.38	1.12 ± 0.15	0.99	0.89	–	–	–	–	72	38	65	81
	EPC/SM/Chol 5:1:1	3.17 ± 0.51	3.17 ± 0.45	2.19	1.53	44.05	56.03	20.12	15.44	76	67	26	9
	EPC/Chol 5:1	3.19 ± 0.53	1.79 ± 0.38	2.34	1.86	43.14	36.90	4.26	17.75	81	79	21	8
	BPS/Chol 5:1	4.73 ± 0.98	1.46 ± 0.78	2.82	2.12	–	–	–	–	25	16	–	–
	Buffer	–	–	10.17	9.18	–	–	–	–	–	–	–	–

mixture, peptide 1A was able of eliciting a significant leakage values compared to peptide 1B (about 70% leakage value for peptide 1A and about 35% for peptide 1B). The leakage values observed for liposomes composed of the negatively charged phospholipids BPS and EPA (BPS/Chol and EPA/Chol at molar ratios of 5:1) were much lower as observed in Fig. 3A and B (leakage values between 5 and 20%). These data show that the interaction of peptides 1A and 1B is significantly higher for liposomes containing mainly zwitterionic phospholipids than negatively charged ones. Although there is no clear relationship between membrane binding and CF leakage, a relatively good relationship exists between the Trp fluorescence intensity of the peptides and CF leakage, i.e., the higher the fluorescence intensity change, the higher the leakage (data not shown). If we suppose that the fluorescence intensity of the Trp residues is related to the peptide location in the membrane [33], the peptides insert more deeply in membranes composed of zwitterionic phospholipids than on membranes composed of negatively charged ones. If that were true, the deeper location of the peptides, the higher the CF leakage is. Peptides 1A and 1B were also able of inducing leakage of fluorophores larger than CF, such as FD10 (Fig. 3C and D). Significant leakage values were observed for liposomes composed of EPC and ER (95–65% maximum leakage values for peptide 1A and 96–80% for peptide 1B). However, leakage values for liposomes composed of EPC/Chol at a molar ratio of 5:1 and EPC/ESM/Chol at a molar ratio of 5:1:1 were very low

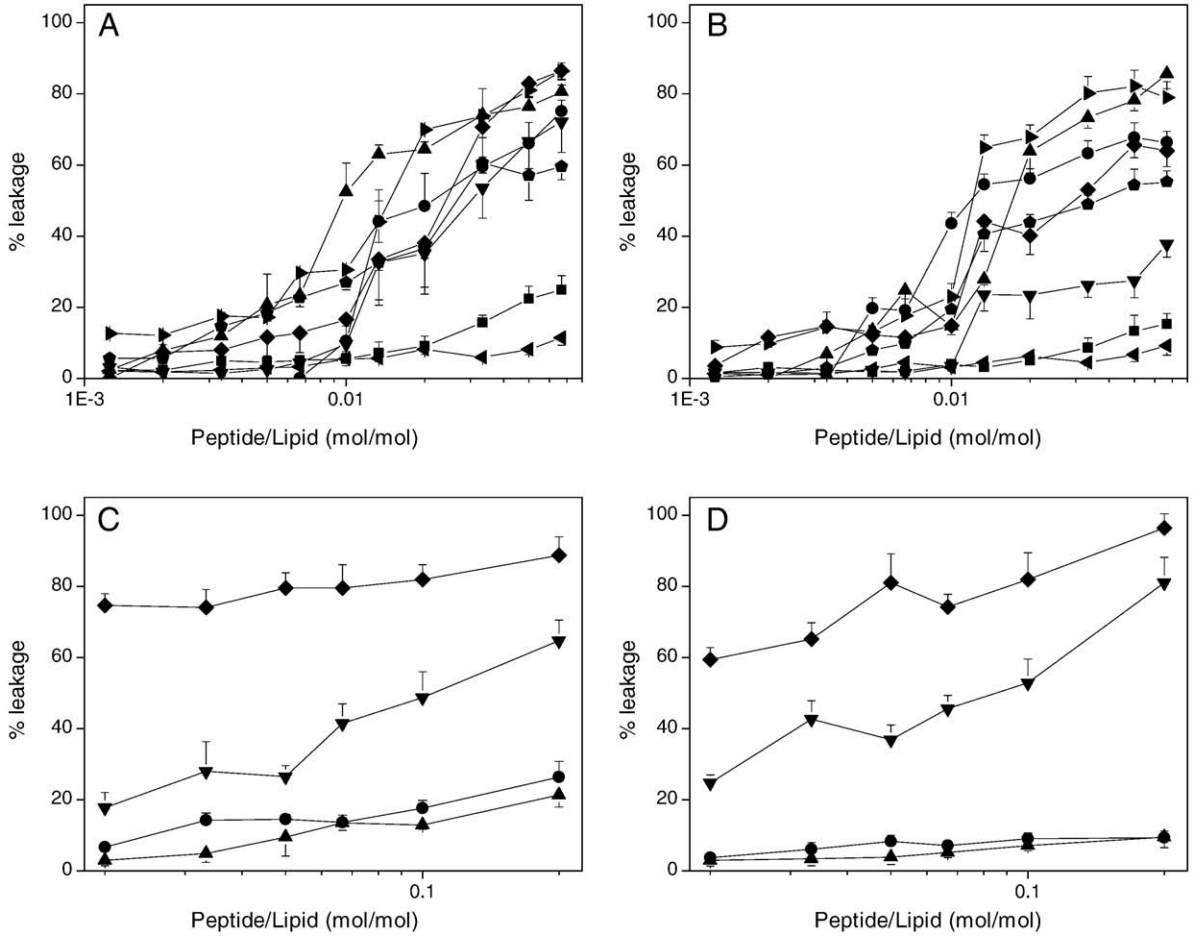

Fig. 3. Effect of the NS5A-derived peptides 1A and 1B on the release (membrane rupture) of CF (A and B) and FD10 (C and D) for different lipid compositions. The lipid compositions used were EPC/ESM/CHOL at a molar ratio of 5:1:1 (●), EPC/CHOL at a molar ratio of 5:1 (▲), synthetic ER membranes (▼), BPS/CHOL at a molar ratio of 5:1 (■), EPC (♦), EPA/CHOL at a molar ratio of 5:1 (◄), EPC/CHOL at a molar ratio of 5:3 (►) and EPC/ESM/CHOL at a molar ratio of 5:3:1(). Vertical bars indicate standard deviations of the mean of triplicate samples.

Please cite this article as: M.F. Palomares-Jerez, et al., Interaction of the N-terminal segment of HCV protein NS5A with model membranes, Biochim. Biophys. Acta (2010), doi:10.1016/j.bbamem.2010.02.007

(maximum leakage values of 20–25% for peptide 1A and 8–9% for peptide 1B), suggesting that Chol decreases the permeability to FD10. As it has been commented previously, this effect could be explained by the effect of Chol on the different location of the peptides (see above), membrane curvature, different peptide translocation and/or peptide aggregation [44]. Therefore peptides 1A and 1B are capable of

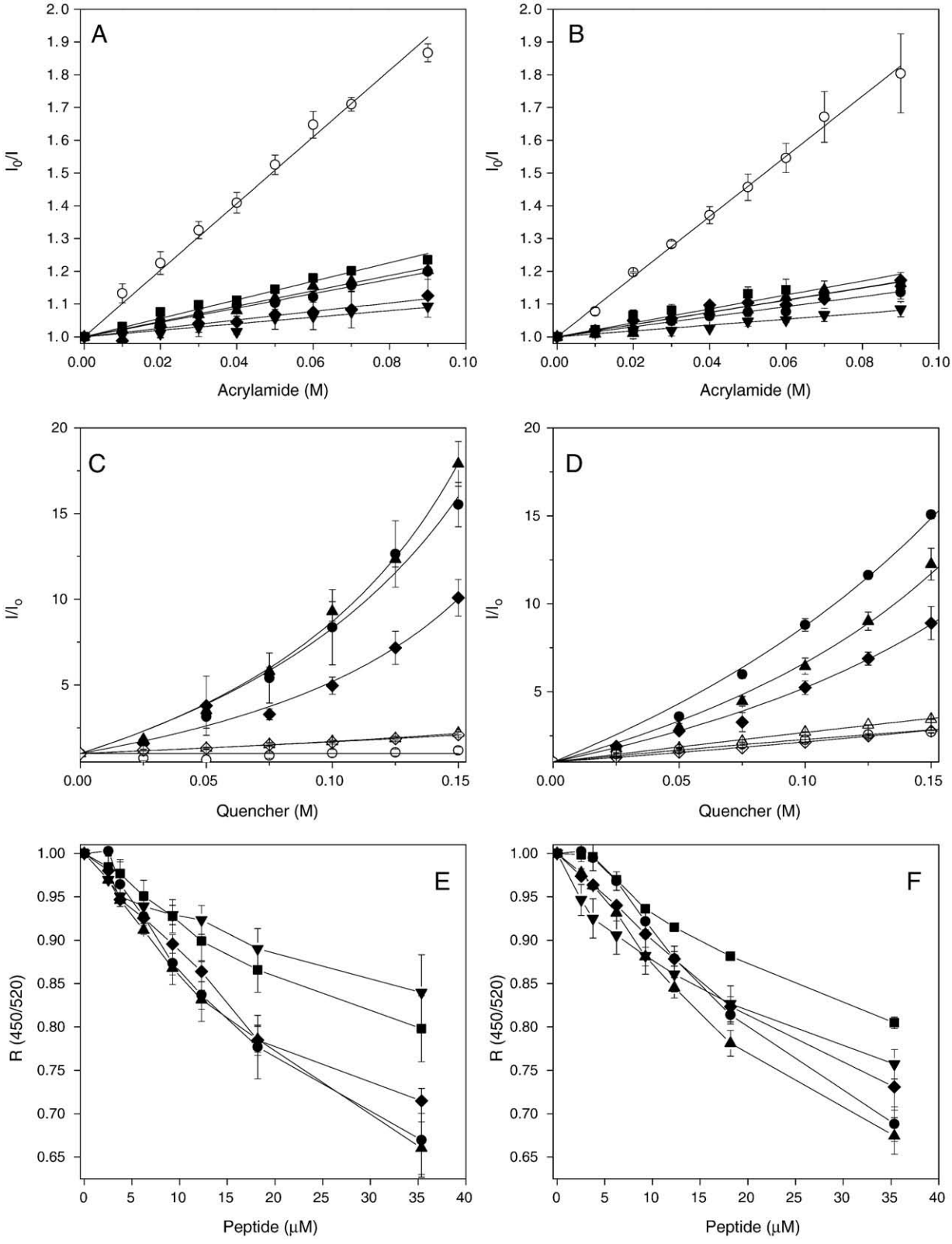

Fig. 4. Stern–Volmer plots for the quenching of the fluorescence of the Trp residues of peptides 1A (A) and 1B (B) by acrylamide, depth-dependent quenching of the Trp fluorescence emission of peptides 1A (C) and 1B (D) by 5-NS (filled symbols) and 16-NS (empty symbols) and effect of peptides 1A (E) and 1B (F) on the membrane dipole potential monitored through the fluorescence ratio (R) of di-8-ANEPPS in the presence of LUVS containing different lipid compositions at different lipid-to-peptide molar ratios. The lipid compositions used were: EPC/ESM/Chol at a molar ratio of 5:1:1 (●), EPC/Chol at a molar ratio of 5:1 (▲), synthetic ER membranes (▼), BPS/Chol at a molar ratio of 5:1 (■), and EPC (♦). Peptides in buffer are represented by (○). The lipid to peptide ratio was 100:1 for the experiments using acrylamide and NS probes.

Please cite this article as: M.F. Palomares-Jerez, et al., Interaction of the N-terminal segment of HCV protein NS5A with model membranes, Biochim. Biophys. Acta (2010), doi:10.1016/j.bbamem.2010.02.007

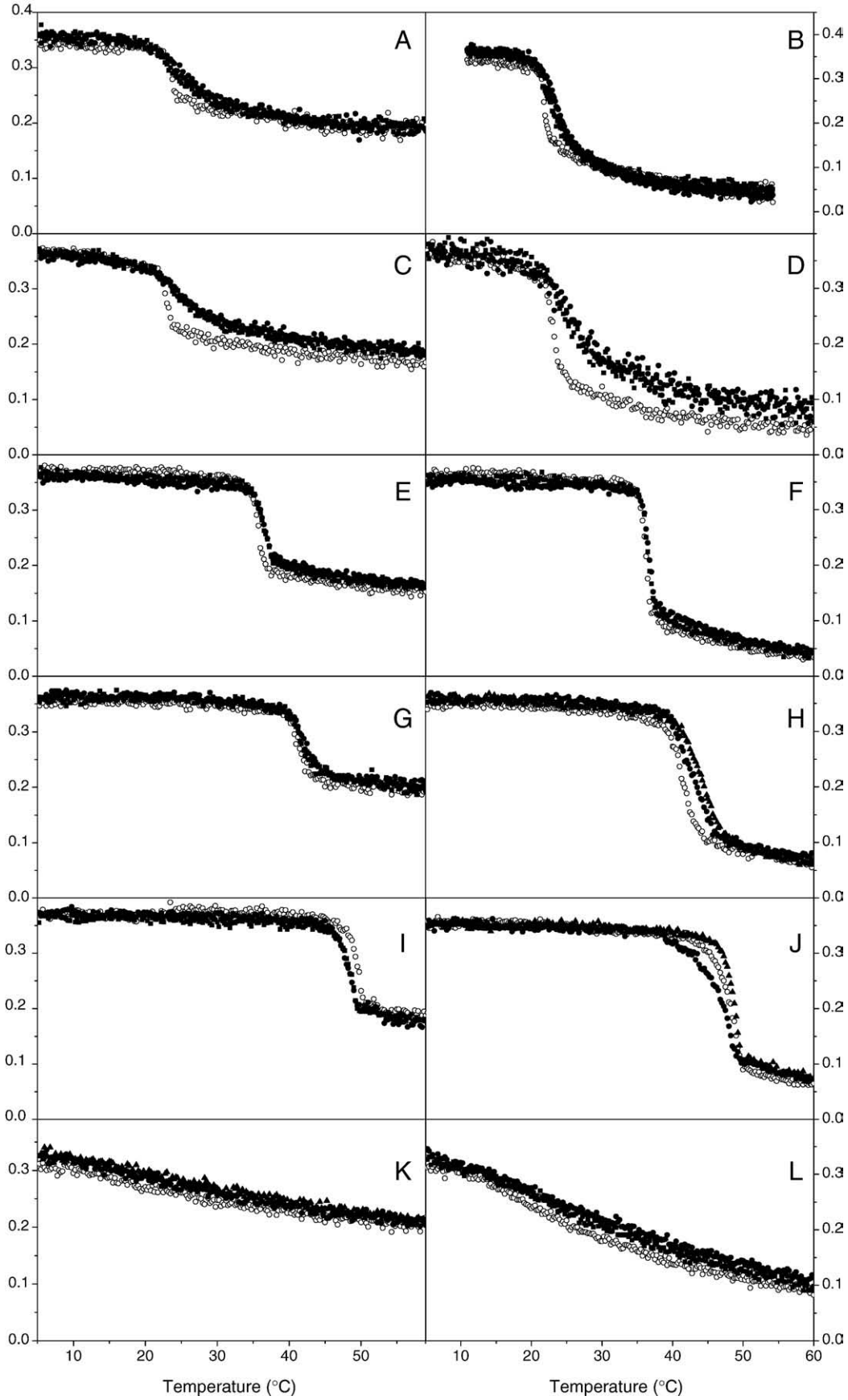

Fig. 5. Steady-state anisotropy, <r>, of TMA-DPH (A, C, E, G, I and K) and DPH (B, D, F, H, J and L) incorporated into (A and B) DMPC, (C and D) DMPG, (E and F) DMPS, (G and H) DPPC, (I and J) DMPA, and (K and L) ER model membranes as a function of temperature. Data correspond to vesicles containing pure phospholipids (○) and phospholipids plus NS5A 1A (●) or 1B (■) derived peptides. The peptide to phospholipid molar ratio was 1:15. The ER complex mixture contained DMPC instead of EPC (see text for details).

Please cite this article as: M.F. Palomares-Jerez, et al., Interaction of the N-terminal segment of HCV protein NS5A with model membranes, Biochim. Biophys. Acta (2010), doi:10.1016/j.bbamem.2010.02.007

forming pores in the membrane, but depending on the lipid composition, a complete disruption of the membrane is attained only at high peptide-to-lipid ratios [45,46].

To investigate the accessibility of the Trp residues of the NS5A 1A and 1B peptides to the aqueous phase in the presence of model membranes, we used acrylamide, an efficient water-soluble neutral quencher probe. Stern–Volmer plots for the quenching of Trp by acrylamide, recorded in the absence and presence of model membranes, are shown in Fig. 4A and B and the resultant Stern–Volmer constants are presented in Table 2. Linear Stern–Volmer plots indicate that the Trp residue is fairly accessible to acrylamide, and in all cases, the quenching of the peptide Trp residue showed an acrylamide dependent concentration behaviour. In aqueous solution the Trp residues were highly exposed to the solvent that led to a more efficient quenching. However, in the presence of the phospholipid membranes, the extent of quenching was significantly reduced, indicating a poor accessibility of the Trp of both peptides to the aqueous phase, consistent with its incorporation into the lipid bilayer. This notion is substantiated by the lower K_{sv} values obtained from the Stern–Volmer plots (Table 2). Significantly, K_{sv} values were similar both in the presence of negatively charged phospholipids and in the presence of zwitterionic ones. The transverse location of the NS5A 1A and 1B peptides into the lipid bilayer was further investigated by monitoring the relative quenching of the Trp fluorescence by the lipophylic spin probes 5-NS and 16-NS. The variation of the fluorescence intensity as a function of the effective concentration of both 5-NS and 16-NS probes is shown in Fig. 4C and D, whereas the K_{sv} values for both probes are presented in Table 2. In general, 16-NS quenches the peptides fluorescence less efficiently than 5-NS, which is consistent with the location of the Trp residues in a shallow position in the membrane. Changes on the membrane dipole potential magnitude elicited by the peptides were monitored by means of the spectral shift of the fluorescence probe di-8-ANEPPS [47]. The variation of the fluorescence intensity ratio $R_{450/520}$ normalized as a function of the peptide concentration for different membrane compositions is shown in Fig. 4E and F. In the presence of the peptides, the greater decrease in the $R_{450/520}$ values were measured in the presence of zwitterionic phospholipids rather than on liposomes composed of negatively charged phospholipids. These data would confirm the presence of a specific interaction of the peptide with vesicles and the peptides were capable of inserting into the lipid bilayer and modifying the dipole potential. Because the NS5A 1A and 1B peptides have a negative net formal charge of −2 and −1 respectively, it is reasonable to assume that an electrostatic repulsion underlies the results obtained with these peptides and the negatively charged phospholipids.

The effect of the NS5A 1A and 1B peptides on the structural and thermotropic properties of phospholipid membranes was also investigated by measuring the steady-state fluorescence anisotropy of the fluorescent probes DPH and TMA-DPH incorporated into model membranes composed of saturated synthetic phospholipids as a function of temperature (Fig. 5). DPH is known to partition mainly into the hydrophobic core of the membrane, whereas TMA-DPH is oriented at the membrane bilayer with its charge localized at the lipid–water interface [48]. Their different locations and orientations in the membrane allow to analyze the effect of the NS5A 1A and 1B peptides on the structural and thermotropic properties along the full length of the membrane. For DMPC, DMPG and DPPC bilayers, the NS5A 1A and 1B peptides decreased slightly the cooperativity of the thermal transition and in addition elicited a shift of about 2–4 °C to higher temperatures of the T_m (Fig. 5A, B, C, D, G and H). However, the anisotropy of both DPH and TMA-DPH above and below the T_m of the phospholipids was not significantly changed. These data suggest that the peptides were able to perturb the phospholipid acyl chains when compared to the pure phospholipids. In contrast, for DMPS we did not observe a significant decrease in cooperativity, although a slight shift of T_m to higher temperatures was evident, more apparent for TMA-DPH than for DPH (Fig. 5E and F). In the case of DMPA there was no significant change in the cooperativity of the transition, although a shift to higher temperatures of the T_m was observed for TMA-DPH (Fig. 5I); however, peptide 1A and peptide 1B induced a shift to lower and higher temperatures respectively in the case of DPH (Fig. 5J). No significant changes in anisotropy were observed below and above the main transition temperature. When the ER complex lipid mixture, having DMPC instead of EPC, was analyzed, the same trend was observed for both probes, i.e., a slight decrease of the cooperativity of the thermal transition and no significant change in the anisotropy both below and above the main transition temperature (Fig. 5K and L). These results suggest that the difference in charge between the phospholipid headgroups affect, but slightly, the peptide incorporation into the lipid bilayer, and therefore it could be suggested that both 1A and 1B peptides, although interacting with the membrane,

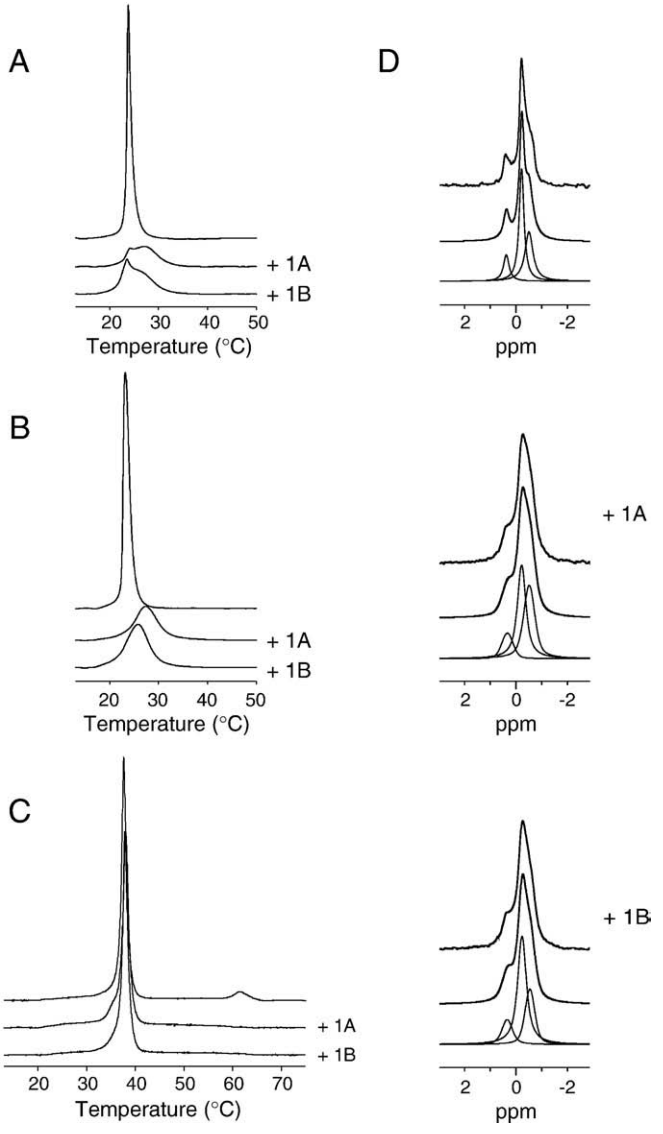

Fig. 6. DSC heating thermograms for model membranes composed of (A) DMPC, (B) DMPG and (C) DEPE in the absence (upper curves) and in the presence of NS5A peptide 1A (middle curve) and peptide 1B (lower curve) at a phospholipid/peptide molar ratio of 15:1. All the thermograms are normalized to the same amount of lipid. (D) MAS ^{31}PNMR at 15 °C and 10 kHz spinning speed (500 MHz proton frequency) spectra for EPC/ESM at a molar ratio of 5:1 multilamellar suspension in the presence of peptides 1A and 1B at a phospholipid/peptide molar ratio of 15:1 as indicated. The original, the fitted envelope and the fitted curves are shown in the upper, middle and lower panels respectively.

Please cite this article as: M.F. Palomares-Jerez, et al., Interaction of the N-terminal segment of HCV protein NS5A with model membranes, Biochim. Biophys. Acta (2010), doi:10.1016/j.bbamem.2010.02.007

should be primarily located at the lipid–water interface influencing the fluidity of the phospholipids [49].

The effect of both NS5A peptides 1A and 1B on the thermotropic phase behaviour of different phospholipid multilamellar vesicles was assayed using differential scanning calorimetry (DSC) and the corresponding profiles are shown in Fig. 6A, B and C. The incorporation of both peptides significantly altered the thermotropic behaviour of both DMPC and DMPG, since the peptides significantly broadened the transition of both phospholipids in accordance with the anisotropy results commented above (Fig. 6A and B). In the case of DMPC and at a lipid/peptide ratio of 15:1, the main transition is apparently associated by at least two different peaks, which should be due to mixed phases (T_m of 24.1 and 27 °C for peptide 1A and 23.6 and 26.1 °C for peptide 1B). The coexistence of at least two phases would indicate that one of them would be enriched in peptide (phospholipids highly disturbed) whereas the other one would be impoverished in them (phospholipids slightly disturbed). In the case of DMPG, the peak is broad but two peaks are not clearly resolvable (T_m of 27.4 °C for peptide 1A and 25.9 °C for peptide 1B). By contrast, both peptides did not broaden significantly the L_β–L_α main transition of DEPE but abolished completely the presence of the lamellar-hexagonal L_α–H_{II} phase transition (Fig. 6C).

We have used ^{31}P MAS NMR to observe the mixture EPC/ESM at a molar ratio of 5:1 since the ^{31}P NMR isotropic chemical shifts of both ESM and EPC headgroups are resolvable under MAS conditions. Furthermore, their spectral intensities reflect the molar ratio of each lipid in the mixture. This approach allows the observation of the line widths of each phospholipid component in the mixture. As observed in Fig. 6D, the chemical shift for the EPC and ESM resonances were not significantly different neither in the absence nor in the presence of both peptides, but the line widths of the ^{31}P resonances of EPC and ESM were dissimilar. Apart from the ESM peak and through the use of fitting, we could distinguish two peaks for the EPC molecule, which comprised about 56% and 44% of the total EPC area (see Fig. 6D). In the absence of peptides, the ^{31}P line width at half height of the EPC resonances was 44 Hz (peak appearing at −0.21 ppm and comprising 39% of the total area) and 75 Hz (peak appearing at −0.58 ppm and comprising 47% of the total area). The ^{31}P line width at half height for the ESM peak was 52 Hz (peak appearing at 0.41 ppm, about 14% of the total area). When peptides 1A and 1B were present, these figures increased to 112 Hz, 81 Hz, 108 Hz and 97 Hz, 84 Hz and 92 Hz respectively. These results show that both phospholipids, EPC and ESM, exhibit a lower degree of mobility and/or an increased heterogeneity of headgroup environments in the presence of peptides 1A and 1B [50].

The existence of structural changes on the NS5A peptides 1A and 1B induced by membrane binding was studied by analyzing the infrared Amide I′ band located between 1700 and 1600 cm^{-1} in membranes by infrared spectroscopy (Fig. 7). The Amide I′ region of the fully hydrated peptides in buffer are shown in Fig. 7A and D. The spectra, at low temperature, are formed by different underlying components that give place to a broad and asymmetric band with maxima at about 1650 cm^{-1} and a shoulder at about 1673 cm^{-1} for peptides 1A and 1B, respectively. At higher temperatures, the maximum of the bands does not change significantly, since they appear at about 1648 cm^{-1} and 1649 cm^{-1} for peptides 1A and 1B, respectively. Interestingly, the band which appear at approximately 1673 cm^{-1} in both peptides 1A and 1B increases in intensity at the same time that temperatures increases (Fig. 1A and D). Significantly, two other bands at about 1685 cm^{-1} and 1616 cm^{-1} appear in the spectra of peptide 1B and increase in intensity as the temperatures is raised (Fig. 7D). The band with the intensity maxima at about 1650 cm^{-1} would correspond to a mixture of unordered but also helical structures, the band at about 1673 cm^{-1} would correspond to β-sheet structures, whereas the bands at about 1685 cm^{-1} and 1616 cm^{-1} appearing at the same time should correspond to aggregated structures [51,52]. These data would imply that peptide 1A changed from a mixture of mainly helical and unordered structures

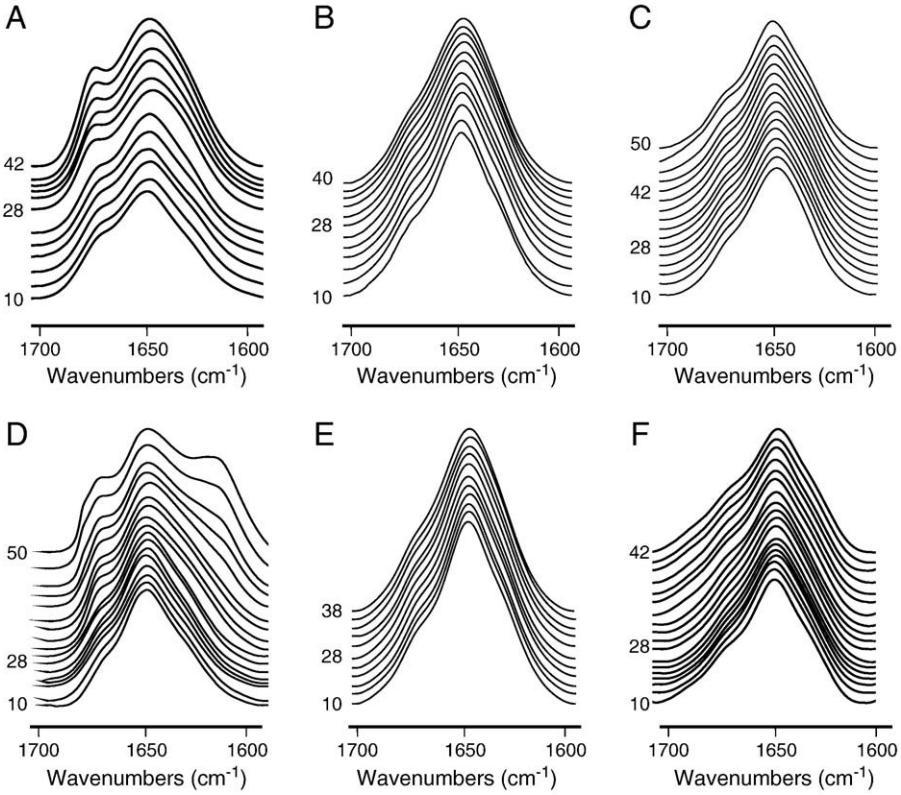

Fig. 7. Stacked infrared spectra in the Amide I′ region of the NS5A-derived peptides 1A (A, B and C) and 1B (D, E and F) in solution (A and D) and in the presence of DMPC (B and E) and DMPG (C and F) at different temperatures as indicated. The phospholipid/peptide molar ratio was 15:1.

Please cite this article as: M.F. Palomares-Jerez, et al., Interaction of the N-terminal segment of HCV protein NS5A with model membranes, Biochim. Biophys. Acta (2010), doi:10.1016/j.bbamem.2010.02.007

at low temperatures to a mixture of helical, unordered and β-sheet structures at high temperatures. However, peptide 1B changed from a mixture of mainly helical and unordered structures at low temperatures to a mixture of aggregated structures and helical, β-sheet and unordered structures at high temperatures. In the presence of both DMPC (Fig. 7B and E) and DMPG (Fig. 7C and F) and at all temperatures studied, the Amide I′ envelope of both NS5A peptides 1A and 1B was rather similar to that found for the peptides in solution at low temperatures. These data would suggest a high degree of conformational stability of the peptides but only in the presence of the model membranes. These results imply that the secondary structure of peptides 1A and 1B was affected by its binding to the membrane.

4. Discussion

The HCV replication process remains largely unclear. The replication and assembly of HCV has been suggested to occur in the endoplasmic reticulum or derived membranes, and it is generally believed that most, if not all, of the NS proteins are involved [6,53,54]. The fact that all NS proteins are localized together with newly synthesized viral RNA on the endoplasmic reticulum or membranes originating from it supports this hypothesis. However, the functions of the individual proteins which participate in the viral replication and/or the assembly remain poorly understood. NS5A is a membrane protein whose function in the HCV life cycle is not known but has a critical role in the HCV life cycle since it has been shown that it is indispensable for replication and assembly [10–12,55,56]. Significantly, genetic disruption of the N-terminal segment of NS5A has been shown to abrogate RNA replication [57], validating this region as a potentially antiviral target.

Since NS5A is associated to the membrane and its function might be modulated by it, we have carried the analysis of the membrane-active regions of NS5A by observing the effect of a NS5A-derived peptide library from HCV strain 1a_H77 on the integrity of two membrane model systems [58]. Following this approach, we have been able of discerning different peptides along the NS5A sequence which display distinct membranotropic properties. When all the membrane leakage values were taken into account, only one region displayed significant membrane rupture activity, namely the sequence encompassing amino acids 3 to 20 (NS5A numbering) (Fig. 1B). Peptide segments 3–20 coincide with the fragment which associates NS5A protein with the membrane and supposedly is implicated in specific protein–protein interactions [15,18]. The importance of this region is demonstrated by the fact that the introduction of mutations into this fragment abolishes HCV RNA replication [19]. Accordingly, we have made a comprehensive study of two peptides patterned after this sequence, peptides 1A and 1B, derived respectively from the NS5A protein sequences from HCV strains 1a_H77 and 1b_HC-J4, characterizing their binding and interaction with model membrane systems through a series of complementary experiments. Our findings give some clues to a key region in the viral protein that might be implicated in the HCV life cycle, and therefore could be used as a new target for searching inhibitors of viral replication and assembly.

Peptides 1A and 1B bind with high affinity to phospholipid model membranes, as it has been similarly found for other peptides [38,41]. An increase in Trp anisotropy was also observed for peptides 1A and 1B in the presence of phospholipid model membranes, showing a significant motional restriction. Binding of peptides 1A and 1B to liposomes was further demonstrated by hydrophilic quenching probes, since both peptides were less accessible for quenching by acrylamide. The peptides decreased the dipole potential of the membrane as well, but in the presence of zwitterionic phospholipid containing model membranes. The fact that the two peptides, as is shown by the fluorescence results, do interact in a similar way with the membrane supports the importance of the specificity on the primary amino acid sequence for the interaction to take effect. The peptide should be located at the lipid–water interface influencing the fluidity of the phospholipids, most probably with an in-plane orientation rather than in a transmembrane position as it has been shown previously [16]. Both peptides were also capable of altering the stability of the membrane, causing the release of fluorescent probes; this effect being dependent on lipid composition and on the lipid/peptide molar ratio. The highest CF release was observed for liposomes containing zwitterionic phospholipids, although significant leakage values were also observed for liposomes composed of negatively charged phospholipids. Interestingly, leakage of fluorophores larger than CF, as FD10, was only observed in liposomes composed of EPC and ER and in lower extent in liposomes containing cholesterol. These differences could be a consequence of influence of cholesterol in the membrane penetration of peptides attenuating its insertion as it has been observed for other peptides [59]. Furthermore, the results obtained in this study suggest that the difference in charge between the phospholipid headgroups affect, the peptide interaction into the lipid bilayer, since the peptides binds to zwitterionic phospholipids with higher affinity and perturbs membrane integrity and dipole potential in a greater extent than those containing negatively charged ones.

We have also shown that both peptides 1A and 1B are capable of affecting the steady-state fluorescence anisotropy of fluorescent probes located into the palisade structure of the membrane, since the peptides decreased the cooperativity of phase transition of saturated phospholipids, without the modification of the mobility of the phospholipid acyl chains neither below nor above it when compared to the pure phospholipids. Additionally, by using MAS NMR, we demonstrated that the phosphate groups of the phospholipid molecules display a lower degree of mobility and/or an increased heterogeneity of the headgroup environment in the presence of both peptides 1A and 1B. This result strengthens that the location of the peptide is at or near the membrane interface. The infrared spectra of the Amide I′ region of the fully hydrated peptides in solution changed significantly with temperature. However, in the presence of membranes no change was observed, demonstrating a high stability of its conformation when bound to the membranes, where a mixture of α-helix, β-sheet and random structures coexisted. These results imply that the secondary structure of the peptides 1A and 1B was affected and stabilized by its binding to the membrane, so that membrane binding modulates the secondary structure of the peptide as it has been suggested for other peptides [38,41,49]. It should be recalled that aggregated structures were only observed for peptide 1B in solution and at relatively high temperatures. This can be due to the change of the disposition of the charged amino acids to locations where they disrupt the hydrophobic surface of the peptide.

Identifying regions within viral proteins is critical to understand and characterize the infection process. The binding to the surface and the modulation of the phospholipid biophysical properties which take place when region comprising amino acids 3 to 20 of HCV NS5A protein is bound to the membrane, i.e., partitioning into the membrane surface and perturbation of the bilayer architecture, could be related to the conformational changes which might occur during the biological activity of the protein. As it has been noted above, a peptide derived from the N-terminal fragment of NS5A and coincidental with peptide 1A has been shown to have potent antiviral activity against HCV and HIV [20,60]. The capacity of peptides derived from this region to bind and modify the structure of membranes must be behind this activity. Therefore, the NS5A region where peptides 1A and 1B reside might have an essential role in the membrane replication and/or assembly of the viral particle through the modulation of the replication complex. Consequently, our findings identify an important region in the HCV NS5A protein which might be directly implicated in the HCV life cycle. Moreover, pharmacological disruption of N-terminal of NS5A interaction with membranes can

Please cite this article as: M.F. Palomares-Jerez, et al., Interaction of the N-terminal segment of HCV protein NS5A with model membranes, Biochim. Biophys. Acta (2010), doi:10.1016/j.bbamem.2010.02.007

represent the basis for a novel approach to anti-HCV therapy. A biophysical methodology similar to the used in the present work could be used for rapid screening of molecules designed with this aim.

Acknowledgements

This work was supported by grant BFU2008-02617-BMC (Ministerio de Ciencia y Tecnología, Spain) to J.V. We are especially grateful to the National Institutes of Health AIDS Research and Reference Reagent Program, Division of AIDS, NIAID, NIH, for the peptides used in this work.

References

[1] Hepatitis C—global prevalence (update), Wkly. Epidemiol. Rec. 75 (2000) 18–19.
[2] S.A. Qureshi, Hepatitis C virus-biology, host evasion strategies, and promising new therapies on the horizon, Med. Res. Rev. 27 (2007) 353–373.
[3] D. Moradpour, F. Penin, C.M. Rice, Replication of hepatitis C virus, Nat. Rev. Microbiol. 5 (2007) 453–463.
[4] C. Vauloup-Fellous, V. Pene, J. Garaud-Aunis, F. Harper, S. Bardin, Y. Suire, E. Pichard, A. Schmitt, P. Sogni, G. Pierron, P. Briand, A.R. Rosenberg, Signal peptide peptidase-catalyzed cleavage of hepatitis C virus core protein is dispensable for virus budding but destabilizes the viral capsid, J. Biol. Chem. 281 (2006) 27679–27692.
[5] M. Hijikata, Y.K. Shimizu, H. Kato, A. Iwamoto, J.W. Shih, H.J. Alter, R.H. Purcell, H. Yoshikura, Equilibrium centrifugation studies of hepatitis C virus: evidence for circulating immune complexes, J. Virol. 67 (1993) 1953–1958.
[6] R. Gosert, D. Egger, V. Lohmann, R. Bartenschlager, H.E. Blum, K. Bienz, D. Moradpour, Identification of the hepatitis C virus RNA replication complex in Huh-7 cells harboring subgenomic replicons, J. Virol. 77 (2003) 5487–5492.
[7] D. Egger, B. Wolk, R. Gosert, L. Bianchi, H.E. Blum, D. Moradpour, K. Bienz, Expression of hepatitis C virus proteins induces distinct membrane alterations including a candidate viral replication complex, J. Virol. 76 (2002) 5974–5984.
[8] D.M. Jones, A.H. Patel, P. Targett-Adams, J. McLauchlan, The hepatitis C virus Ns4b protein can trans-complement viral RNA replication and modulates production of infectious virus, J. Virol. 83 (2009) 2163–2177.
[9] M. Dimitrova, I. Imbert, M.P. Kieny, C. Schuster, Protein–protein interactions between hepatitis C virus nonstructural proteins, J. Virol. 77 (2003) 5401–5414.
[10] S.L. Tan, M.G. Katze, How hepatitis C virus counteracts the interferon response: the jury is still out on NS5A, Virology 284 (2001) 1–12.
[11] T.L. Tellinghuisen, K.L. Foss, J. Treadaway, Regulation of hepatitis C virion production via phosphorylation of the NS5A protein, PLoS Pathog. 4 (2008) e1000032.
[12] T. Masaki, R. Suzuki, K. Murakami, H. Aizaki, K. Ishii, A. Murayama, T. Date, Y. Matsuura, T. Miyamura, T. Wakita, T. Suzuki, Interaction of hepatitis C virus nonstructural protein 5A with core protein is critical for the production of infectious virus particles, J. Virol. 82 (2008) 7964–7976.
[13] U. Schmitz, S.L. Tan, NS5A—from obscurity to new target for HCV therapy, Recent Patents Anti-Infect. Drug Disc. 3 (2008) 77–92.
[14] T. Suzuki, K. Ishii, H. Aizaki, T. Wakita, Hepatitis C viral life cycle, Adv. Drug Deliv. Rev. 59 (2007) 1200–1212.
[15] T.L. Tellinghuisen, J. Marcotrigiano, A.E. Gorbalenya, C.M. Rice, The NS5A protein of hepatitis C virus is a zinc metalloprotein, J. Biol. Chem. 279 (2004) 48576–48587.
[16] F. Penin, V. Brass, N. Appel, S. Ramboarina, R. Montserret, D. Ficheux, H.E. Blum, R. Bartenschlager, D. Moradpour, Structure and function of the membrane anchor domain of hepatitis C virus nonstructural protein 5A, J. Biol. Chem. 279 (2004) 40835–40843.
[17] V. Brass, E. Bieck, R. Montserret, B. Wolk, J.A. Hellings, H.E. Blum, F. Penin, D. Moradpour, An amino-terminal amphipathic alpha-helix mediates membrane association of the hepatitis C virus nonstructural protein 5A, J. Biol. Chem. 277 (2002) 8130–8139.
[18] N. Sapay, R. Montserret, C. Chipot, V. Brass, D. Moradpour, G. Deleage, F. Penin, NMR structure and molecular dynamics of the in-plane membrane anchor of nonstructural protein 5A from bovine viral diarrhea virus, Biochemistry 45 (2006) 2221–2233.
[19] N.J. Cho, S.J. Cho, J.O. Hardesty, J.S. Glenn, C.W. Frank, Creation of lipid partitions by deposition of amphipathic viral peptides, Langmuir 23 (2007) 10855–10863.
[20] G. Cheng, A. Montero, P. Gastaminza, C. Whitten-Bauer, S.F. Wieland, M. Isogawa, B. Fredericksen, S. Selvarajah, P.A. Gallay, M.R. Ghadiri, F.V. Chisari, A virocidal amphipathic {alpha}-helical peptide that inhibits hepatitis C virus infection in vitro, Proc. Natl. Acad. Sci. U. S. A. 105 (2008) 3088–3093.
[21] A.J. Perez-Berna, J. Guillen, M.R. Moreno, A. Bernabeu, G. Pabst, P. Laggner, J. Villalain, Identification of the membrane-active regions of hepatitis C virus p7 protein: biophysical characterization of the loop region, J. Biol. Chem. 283 (2008) 8089–8101.
[22] A.J. Perez-Berna, A.S. Veiga, M.A. Castanho, J. Villalain, Hepatitis C virus core protein binding to lipid membranes: the role of domains 1 and 2, J. Viral Hepatitis 15 (2008) 346–356.
[23] A.J. Perez-Berna, G. Pabst, P. Laggner, J. Villalain, Biophysical characterization of the fusogenic region of HCV envelope glycoprotein E1, Biochim. Biophys. Acta 1788 (2009) 2183–2193.
[24] W.K. Surewicz, H.H. Mantsch, D. Chapman, Determination of protein secondary structure by Fourier transform infrared spectroscopy: a critical assessment, Biochemistry 32 (1993) 389–394.
[25] Y.P. Zhang, R.N. Lewis, R.S. Hodges, R.N. McElhaney, FTIR spectroscopic studies of the conformation and amide hydrogen exchange of a peptide model of the hydrophobic transmembrane alpha-helices of membrane proteins, Biochemistry 31 (1992) 11572–11578.
[26] A.G. Krainev, D.A. Ferrington, T.D. Williams, T.C. Squier, D.J. Bigelow, Adaptive changes in lipid composition of skeletal sarcoplasmic reticulum membranes associated with aging, Biochim. Biophys. Acta 1235 (1995) 406–418.
[27] L.D. Mayer, M.J. Hope, P.R. Cullis, Vesicles of variable sizes produced by a rapid extrusion procedure, Biochim. Biophys. Acta 858 (1986) 161–168.
[28] C.S.F. Böttcher, C.M. VanGent, C. Fries, A rapid and sensitive sub-micro phosphorus determination, Anal. Chim. Acta 1061 (1961) 203–204.
[29] H. Edelhoch, Spectroscopic determination of tryptophan and tyrosine in proteins, Biochemistry 6 (1967) 1948–1954.
[30] A. Bernabeu, J. Guillen, A.J. Perez-Berna, M.R. Moreno, J. Villalain, Structure of the C-terminal domain of the pro-apoptotic protein Hrk and its interaction with model membranes, Biochim. Biophys. Acta 1768 (2007) 1659–1670.
[31] M.R. Moreno, J. Guillen, A.J. Perez-Berna, D. Amoros, A.I. Gomez, A. Bernabeu, J. Villalain, Characterization of the interaction of two peptides from the N terminus of the NHR domain of HIV-1 gp41 with phospholipid membranes, Biochemistry 46 (2007) 10572–10584.
[32] B. Sainz Jr., J.M. Rausch, W.R. Gallaher, R.F. Garry, W.C. Wimley, Identification and characterization of the putative fusion peptide of the severe acute respiratory syndrome-associated coronavirus spike protein, J. Virol. 79 (2005) 7195–7206.
[33] J. Lakowicz, Principles of Fluorescence Spectroscopy, Kluwer-Plenum Press, New York, 1999.
[34] J. Cladera, P. O'Shea, Intramembrane molecular dipoles affect the membrane insertion and folding of a model amphiphilic peptide, Biophys. J. 74 (1998) 2434–2442.
[35] E. Gross, R.S. Bedlack Jr., L.M. Loew, Dual-wavelength ratiometric fluorescence measurement of the membrane dipole potential, Biophys. J. 67 (1994) 208–216.
[36] J. Guillen, M.R. Moreno, A.J. Perez-Berna, A. Bernabeu, J. Villalain, Interaction of a peptide from the pre-transmembrane domain of the severe acute respiratory syndrome coronavirus spike protein with phospholipid membranes, J. Phys. Chem. B 111 (2007) 13714–13725.
[37] V. Brass, Z. Pal, N. Sapay, G. Deleage, H.E. Blum, F. Penin, D. Moradpour, Conserved determinants for membrane association of nonstructural protein 5A from hepatitis C virus and related viruses, J. Virol. 81 (2007) 2745–2757.
[38] R. Pascual, M. Contreras, A. Fedorov, M. Prieto, J. Villalain, Interaction of a peptide derived from the N-heptad repeat region of gp41 Env ectodomain with model membranes. Modulation of phospholipid phase behavior, Biochemistry 44 (2005) 14275–14288.
[39] H. Aizaki, K.J. Lee, V.M. Sung, H. Ishiko, M.M. Lai, Characterization of the hepatitis C virus RNA replication complex associated with lipid rafts, Virology 324 (2004) 450–461.
[40] S.T. Shi, K.J. Lee, H. Aizaki, S.B. Hwang, M.M. Lai, Hepatitis C virus RNA replication occurs on a detergent-resistant membrane that cofractionates with caveolin-2, J. Virol. 77 (2003) 4160–4168.
[41] R. Pascual, M.R. Moreno, J. Villalain, A peptide pertaining to the loop segment of human immunodeficiency virus gp41 binds and interacts with model biomembranes: implications for the fusion mechanism, J. Virol. 79 (2005) 5142–5152.
[42] T.C. Laurent, K.A. Granath, Fractionation of dextran and Ficoll by chromatography on Sephadex G-200, Biochim. Biophys. Acta 136 (1967) 191–198.
[43] D.B. Fisher, C.E. Cash-Clark, Sieve tube unloading and post-phloem transport of fluorescent tracers and proteins injected into sieve tubes via severed aphid stylets, Plant Physiol. 123 (2000) 125–138.
[44] S. Nir, J.L. Nieva, Interactions of peptides with liposomes: pore formation and fusion, Prog. Lipid Res. 39 (2000) 181–206.
[45] L. Yang, T.A. Harroun, T.M. Weiss, L. Ding, H.W. Huang, Barrel-stave model or toroidal model? A case study on melittin pores, Biophys. J. 81 (2001) 1475–1485.
[46] D. Allende, S.A. Simon, T.J. McIntosh, Melittin-induced bilayer leakage depends on lipid material properties: evidence for toroidal pores, Biophys. J. 88 (2005) 1828–1837.
[47] P. O'Shea, Intermolecular interactions with/within cell membranes and the trinity of membrane potentials: kinetics and imaging, Biochem. Soc. Trans. 31 (2003) 990–996.
[48] B.R. Lentz, Use of fluorescent probes to monitor molecular order and motions within liposome bilayers, Chem. Phys. Lipids 64 (1993) 99–116.
[49] L.M. Contreras, F.J. Aranda, F. Gavilanes, J.M. Gonzalez-Ros, J. Villalain, Structure and interaction with membrane model systems of a peptide derived from the major epitope region of HIV protein gp41: implications on viral fusion mechanism, Biochemistry 40 (2001) 3196–3207.
[50] G.P. Holland, S.K. McIntyre, T.M. Alam, Distinguishing individual lipid headgroup mobility and phase transitions in raft-forming lipid mixtures with 31P MAS NMR, Biophys. J. 90 (2006) 4248–4260.
[51] J.L. Arrondo, F.M. Goni, Structure and dynamics of membrane proteins as studied by infrared spectroscopy, Prog. Biophys. Mol. Biol. 72 (1999) 367–405.
[52] D.M. Byler, H. Susi, Examination of the secondary structure of proteins by deconvolved FTIR spectra, Biopolymers 25 (1986) 469–487.
[53] N. El-Hage, G. Luo, Replication of hepatitis C virus RNA occurs in a membrane-bound replication complex containing nonstructural viral proteins and RNA, J. Gen. Virol. 84 (2003) 2761–2769.
[54] G. Mottola, G. Cardinali, A. Ceccacci, C. Trozzi, L. Bartholomew, M.R. Torrisi, E. Pedrazzini, S. Bonatti, G. Migliaccio, Hepatitis C virus nonstructural proteins are

Please cite this article as: M.F. Palomares-Jerez, et al., Interaction of the N-terminal segment of HCV protein NS5A with model membranes, Biochim. Biophys. Acta (2010), doi:10.1016/j.bbamem.2010.02.007

localized in a modified endoplasmic reticulum of cells expressing viral subgenomic replicons, Virology 293 (2002) 31–43.
[55] M.J. Gale Jr., M.J. Korth, N.M. Tang, S.L. Tan, D.A. Hopkins, T.E. Dever, S.J. Polyak, D. R. Gretch, M.G. Katze, Evidence that hepatitis C virus resistance to interferon is mediated through repression of the PKR protein kinase by the nonstructural 5A protein, Virology 230 (1997) 217–227.
[56] N. Enomoto, I. Sakuma, Y. Asahina, M. Kurosaki, T. Murakami, C. Yamamoto, Y. Ogura, N. Izumi, F. Marumo, C. Sato, Mutations in the nonstructural protein 5A gene and response to interferon in patients with chronic hepatitis C virus 1b infection, N. Engl. J. Med. 334 (1996) 77–81.
[57] M. Elazar, K.H. Cheong, P. Liu, H.B. Greenberg, C.M. Rice, J.S. Glenn, Amphipathic helix-dependent localization of NS5A mediates hepatitis C virus RNA replication, J. Virol. 77 (2003) 6055–6061.
[58] J. Guillen, A. Gonzalez-Alvarez, J. Villalain, A membranotropic region in the C-terminal domain of hepatitis C virus protein NS4B interaction with membranes, Biochim. Biophys. Acta (in press), doi:10.1016/j.bbamem.2009.07.011.
[59] H. Zhao, R. Sood, A. Jutila, S. Bose, G. Fimland, J. Nissen-Meyer, P.K. Kinnunen, Interaction of the antimicrobial peptide pheromone Plantaricin A with model membranes: implications for a novel mechanism of action, Biochim. Biophys. Acta 1758 (2006) 1461–1474.
[60] M.D. Bobardt, G. Cheng, L. de Witte, S. Selvarajah, U. Chatterji, B.E. Sanders-Beer, T.B. Geijtenbeek, F.V. Chisari, P.A. Gallay, Hepatitis C virus NS5A anchor peptide disrupts human immunodeficiency virus, Proc. Natl. Acad. Sci. U. S. A. 105 (2008) 5525–5530.
[61] T.L. Tellinghuisen, K.L. Foss, J.C. Treadaway, C.M. Rice, Identification of residues required for RNA replication in domains II and III of the hepatitis C virus NS5A protein, J. Virol. 82 (2008) 1073–1083.

Please cite this article as: M.F. Palomares-Jerez, et al., Interaction of the N-terminal segment of HCV protein NS5A with model membranes, Biochim. Biophys. Acta (2010), doi:10.1016/j.bbamem.2010.02.007